

Algebraic Representations for Faster Predictions in Convolutional Neural Networks*

Johnny Joyce[†] Jan Vershelde[‡]

August 16, 2024

Abstract

Convolutional neural networks (CNNs) are a popular choice of model for tasks in computer vision. When CNNs are made with many layers, resulting in a *deep* neural network, skip connections may be added to create an easier gradient optimization problem while retaining model expressiveness. In this paper, we show that arbitrarily complex, trained, linear CNNs with skip connections can be simplified into a single-layer model, resulting in greatly reduced computational requirements during prediction time. We also present a method for training nonlinear models with skip connections that are gradually removed throughout training, giving the benefits of skip connections without requiring computational overhead during prediction time. These results are demonstrated with practical examples on Residual Networks (ResNet) architecture.

Keywords and phrases. Skip connections, linear convolutional networks, ResNet.

1 Introduction

Convolutional neural networks (CNNs) are a type of multi-layer neural network that primarily utilize convolution (cross-correlation) operations, as opposed to regular neural networks (NNs), which utilize fully-connected layers.

*Supported by the National Science Foundation under grant DMS 1854513.

[†]University of Illinois at Chicago, Department of Mathematics, Statistics, and Computer Science, 851 S. Morgan St. (m/c 249), Chicago, IL 60607-7045, U.S.A. Email: jjoyce22@uic.edu, URL: <https://jjoyce22.people.uic.edu/>.

[‡]University of Illinois at Chicago, Department of Mathematics, Statistics, and Computer Science, 851 S. Morgan St. (m/c 249), Chicago, IL 60607-7045, U.S.A. Email: janv@uic.edu, URL: <http://www.math.uic.edu/~jan>.

Like fully-connected layers, convolutions can be represented as transformation matrices [10], but possess different properties that make them well-suited for tasks involving images and videos, such as classification and segmentation.

CNNs, along with other types of neural networks, have the ability to represent functions whose complexity grows exponentially as the number of layers in the network increases [17]. *Deep* neural networks, which consist of many layers, therefore offer great performance enhancements over their shallow counterparts, but are more difficult to train if considerations are not made on how to account for this tradeoff. *Skip connections* (or shortcut connections or residual connections) help make NNs easier to train — these work by taking the output of a particular layer, then adding it to the input of some later layer. That is, if a neural network takes input X , and the i^{th} layer computes $f(X)$, and the $(j - 1)^{\text{th}}$ layer computes $g(X)$, then a skip connection from layer i to layer j gives $f(X) + g(X)$ as the input to the j^{th} layer. A famous example of a model that uses skip connections is **ResNet** [6], whose common variants may have up to 152 layers, and have won various machine learning competitions.

Generally speaking, skip connections allow for the training process to be an easier optimization problem by retaining information as it moves throughout the network and by allowing gradients to backpropagate through the network more easily, mitigating the ‘vanishing gradients’ problem. More specific explanations are available, such as that they remove singularities in the loss landscape [15], but a full algebraic explanation has not yet been formulated.

1.1 machine learning and algebraic geometry

Algebraic geometry has been used in various ways to analyze neural networks (NNs) and machine learning in general. In 2018, Zhang et al [22] made connections between NNs and tropical geometry by showing that NNs with ReLU activation functions can be represented as tropical signomial maps. Using this connection, they gave bounds on number of regions of a NN’s decision boundary, showed that zonotopes form “building blocks” of NNs under a tropical geometry view, and showed that the expressiveness of NNs grows exponentially with the number of layers. This sparked interest in this recent field was surveyed by Maragos et al in 2022 [14].

Algebraic interpretations of neural networks have also taken different approaches. In 2022, Kohn et al [10] examined the function space of linear CNNs, concluding that training a linear CNN with gradient descent results in a bias towards repeated filters that are not globally optimal. This, along

with other examples [11, 9], is one example of a deep field of work where the loss landscape of NNs is examined — a topic that is also often the focus of *singular learning theory*. One such work by Hardt and Ma in 2017 [5] directly uses such an analysis of loss landscapes to show that deep residual neural networks, which use skip connections, have no critical points other than global minima.

Singular learning theory is another approach that provides rich connections between algebraic geometry, as explored in great detail in Watanabe’s 2009 book [19]. Examples of important results from this field include that almost all learning machines (NNs, mixture models, etc) are singular, so regular statistical learning theory does not apply [18] (thereby motivating why analyzing NNs is important); and that optimizing Bayes cross-validation is equivalent to optimizing another criterion used in singular learning theory [20]. Such work allowed for exact computation of marginal likelihood integrals (model evidence) for certain models [13] where otherwise it would have usually been approximated.

CNNs, skip connections (as in residual NNs), and singularities were tied together by Orhan and Pitkow in 2018 [15], who showed that the use of skip connections in a CNN avoids singularities previously analyzed by Wei et al [21]. However, it should be noted that this approach does not *resolve* existing singularities (e.g. as one would by applying techniques like successive blow-ups), but instead demonstrates that architectures with skip connections are not subject to singularities in the first place, thereby differing from approaches like those of Watanabe in singular learning theory. Conversely, the other direction has been explored, with NNs having been used to; resolve singularities [2], analyze algebraic structures [1], solve problems in ways inspired by algebraic geometric methods [8], and solve problems while maintaining awareness of singularities [7]. Symbolic computation also has rich connections with machine learning, including the use of polynomials to analyze neural networks [10], and applied machine learning to assist in symbolic computation [3, 16].

1.2 contributions and structure

The structure of the remainder of this paper is as follows:

- In Section 2, we introduce a setup and relevant terminology for *linear* CNNs (LCNs), with emphasis on viewing convolutions as transformation matrices.
- In Section 3, we add the necessary framework for skip connections to

our setup and present a theorem that allows for the prediction function arbitrarily complex trained LCNs with skip connections to be pre-calculated. This facilitates the creation of models with strong performance on image-related tasks that only require the resources of a single-layer perceptron when making predictions. This can give an arbitrarily high speedup factor — in the case of a linearized version of ResNet34, we observe a speedup of 98%.

- In Section 4, we expand our view to include nonlinear CNNs, and present a method for removing skip connections, resulting in an observed 22% to 46% speedup in prediction time in practical experiments.
- In Section 4, we conclude by exploring potential future research directions based on our results.

All code used in this paper’s experiments is available in a Jupyter Notebook file stored a public GitHub repository ¹.

2 CNN setup

In this section, we describe a setup for *feed-forward* CNNs — we use feed-forward to distinguish networks that do not contain skip connections. This setup is similar to that of Kohn et al. [10], who describe 1-dimensional convolutions as Toeplitz matrices. Our setup for this section differs from that of Kohn et al. in the following ways; we focus on 2-dimensional (or higher) inputs and represent them as 1-dimensional vectors, we focus primarily on classification rather than regression (though this setup can also be applied to regression), and we assume that all convolution operations are immediately followed by adding a corresponding bias vector. Furthermore, we will expand upon this setup in Section 3 to allow for skip connections, facilitating the use of much larger and deeper neural networks.

We start with a basic CNN architecture consisting of $L - 1$ convolutional layers, followed by a single fully-connected layer. For each convolutional layer, indexed by $i = 1, \dots, L - 1$, we use $\alpha^{(i)}$ to refer to the layer as a function from its input space to its output space, $K^{(i)}$ to refer to its kernel, its stride as $s^{(i)}$, and its bias as $B^{(i)}$. The fully-connected layer $\alpha^{(L)}$ allows us to perform classification by mapping the output of the final convolutional layer to a vector of size C , where C corresponds to the number of class

¹<https://github.com/johnnyvjoyce/simplify-skip-connections>

labels. For each $i \in \{1, \dots, C\}$ the i^{th} entry of the output corresponds to the probability that the input is associated with the i th class.

It is common to use a *softmax* activation function after the final layer (which maps the output vector to a probability distribution), but to maintain linearity, we instead treat the softmax layer as part of the loss function. This does not change the optimization problem, and therefore has no positive or negative effect on model performance.

Inputs to our CNN are two-dimensional grayscale images, which would ordinarily be best represented by a $(h \times w)$ -matrix M containing saturation values ranging from 0 (black) to 1 (white). However, our notation and calculations involving convolutions are made simpler if we first “unravel” our input into a vector X of size hw , where $X_i = M_{(\lfloor i/w \rfloor, i \bmod w)}$ for all $i \in \{1, \dots, hw\}$. We may also use color images in RGB format, which would contain 3 saturation values for each pixel — one for each of red, green, and blue. This scenario is analogous, but requires unraveling a tensor of rank 3 rather than a matrix. We can take arbitrarily high input dimensions for other scenarios by unravelling in this way if needed.

With this setup, we can view all of the CNN’s layers $\{\alpha^{(i)} : i = 1, \dots, n\}$ as affine maps $\alpha^{(i)}(x) = W^{(i)}X + B^{(i)}$ — the convolutional layers are viewed as Toeplitz matrices, while the fully-connected layer keeps its usual representation. The CNN can then be represented as a map $f(X) = (\alpha^{(n)} \circ \dots \circ \alpha^{(1)})(X)$. Furthermore, we have the following:

$$f(X) = (\alpha^{(L)} \circ \dots \circ \alpha^{(1)})(X) \quad (1)$$

$$= W^{(L)}(\dots (W^{(2)}(W^{(1)}X + B^{(1)}) + B^{(2)}) \dots) + B^{(L)} \quad (2)$$

$$= W^{(L)}(\dots (W^{(2)}W^{(1)}X + W^{(2)}B^{(1)} + B^{(2)}) \dots) + B^{(L)} \quad (3)$$

$$= \left(W^{(L)} \dots W^{(2)}W^{(1)} \right) X + \left((W^{(L)} \dots W^{(2)})B^{(1)} + \dots + W^{(2)}B^{(n-1)} + B^{(L)} \right) \quad (4)$$

$$= \left(\prod_{i=1}^L W^{(i)} \right) X + \sum_{i=1}^L \left(\left(\prod_{j=i+1}^L W^{(j)} \right) B^{(i)} \right) \quad (5)$$

Hence $f(X)$ is itself an affine map, given by $f(X) = WX + B$, where $W := \prod_{i=1}^L W^{(i)}$ and $B := \sum_{i=1}^L \left(\left(\prod_{j=i+1}^L W^{(j)} \right) B^{(i)} \right)$ (where \prod uses left-multiplication of successive matrices).

We may also consider the map $g := \alpha^{(n-1)} \circ \dots \circ \alpha^{(1)}$, which consists of all convolutional layers, with the final fully-connected layer removed. This is a map from our inputs into *latent space*, which is a lower-dimensional representation of the original inputs. We have that g is also an affine map, given by $g(X) = W_{\text{latent}}X + B_{\text{latent}}$, where $W_{\text{latent}} := \prod_{i=1}^{n-1} W^{(i)}$ and

$$B_{\text{latent}} := \sum_{i=1}^{L-1} \left(\prod_{j=i+1}^{L-1} W^{(j)} \right) B^{(i)}.$$

3 Skip Connections in Linear Networks

Skip connections add the outputs of multiple layers together as information moves through a neural network. To achieve this, the operands for these tensor addition operations must be the same size. However, convolutional layers in a CNN *reduce* the size of an image if no counteractive measures are taken.

Therefore, we introduce *resampling* and *padding* in Section 3.1, both of which allow for the loss in size when using convolutions to be counteracted, making them a necessary prerequisite for adding skip connections. These are both standard operations in machine learning, but we show them to emphasize a somewhat uncommon approach of representing them as transformation matrices. In Section 3.2, we utilize these transformation matrices to create a network with skip connections.

Though padding and resampling both achieve similar goals, they provide different and complementary utility. Padding an image before performing a convolution ensures that the output of the convolution has the same size as the input before padding — a CNN that only utilizes padding will therefore perform successive convolutions on an image that retains its size. On the other hand, resampling allows us to explicitly choose the size of the input, making it either smaller or larger — a CNN that only utilizes resampling will have inputs that get smaller as successive convolutions are applied. By manipulating the size of the image as it passes through layers, we can alter the *receptive field* of the network.

3.1 Transformation matrices for resampling and padding

Take a (2×2) -matrix $A := \begin{bmatrix} a_{1,1} & a_{1,2} \\ a_{2,1} & a_{2,2} \end{bmatrix}$. Each of the entries have been assigned an arbitrary color for ease of visualizing this matrix as an image.

3.1.1 Resampling.

Suppose we want to resample A into a (3×4) -matrix using nearest-neighbor interpolation. To achieve this, we first need to reshape A into a (4×1) column vector. We can then use the transformation matrix shown on the left-hand side of (6) to obtain the (12×1) column vector shown on the right-hand side of (6).

$$\begin{bmatrix} 1 & 0 & 0 & 0 \\ 1 & 0 & 0 & 0 \\ 0 & 1 & 0 & 0 \\ 0 & 1 & 0 & 0 \\ 0 & 0 & 1 & 0 \\ 0 & 0 & 1 & 0 \\ 0 & 0 & 0 & 1 \\ 0 & 0 & 0 & 1 \\ 0 & 0 & 1 & 0 \\ 0 & 0 & 1 & 0 \\ 0 & 0 & 0 & 1 \\ 0 & 0 & 0 & 1 \end{bmatrix} \cdot \begin{bmatrix} a_{1,1} \\ a_{1,2} \\ a_{2,1} \\ a_{2,2} \end{bmatrix} = \begin{bmatrix} a_{1,1} \\ a_{1,1} \\ a_{1,2} \\ a_{1,2} \\ a_{2,1} \\ a_{2,1} \\ a_{2,2} \\ a_{2,2} \\ a_{2,1} \\ a_{2,1} \\ a_{2,2} \\ a_{2,2} \end{bmatrix} \quad (6)$$

Finally, by reshaping the resulting column vector into a (3×4) -matrix, we obtain:

$$B = \begin{bmatrix} a_{1,1} & a_{1,1} & a_{1,2} & a_{1,2} \\ a_{2,1} & a_{2,1} & a_{2,2} & a_{2,2} \\ a_{2,1} & a_{2,1} & a_{2,2} & a_{2,2} \end{bmatrix} \quad (7)$$

By comparing the colors of the original matrix A against the colors of the result B , we can see that this resampling has preserved the positions of matrix entries as they would appear if they were pixels in an image.

In this example, the second row of B contains entries from the final row of A , but an equally valid approach could have been to take these entries from the first row of A . Alternatively, if we wished to instead use a more complex resampling method, such as bilinear interpolation, we could achieve this by changing the entries of our transformation matrix in (6).

For simplicity, we use nearest-neighbor interpolation in our experiments, and for consistency, entries of our resampling matrix are found through coordinate transforms in a way that matches the implementation of the common Python packages Pillow, scikit-image, and PyTorch.

3.1.2 Padding.

Another common technique in CNNs is *padding*, where a border is introduced around the edges of an image. These borders may consist of zeros, samples of pixels near the border, or other methods.

For example, if we use the sample example matrix A as in Section 3.1.1 and reshape it into a vector in the same way, we can pad A with a border of zeros of size 1 with the following transformation matrix:

$$\begin{bmatrix} 0 & 0 & 0 & 0 \\ 0 & 0 & 0 & 0 \\ 0 & 0 & 0 & 0 \\ 0 & 0 & 0 & 0 \\ 0 & 0 & 0 & 0 \\ 1 & 0 & 0 & 0 \\ 0 & 1 & 0 & 0 \\ 0 & 0 & 0 & 0 \\ 0 & 0 & 0 & 0 \\ 0 & 0 & 1 & 0 \\ 0 & 0 & 0 & 1 \\ 0 & 0 & 0 & 0 \\ 0 & 0 & 0 & 0 \\ 0 & 0 & 0 & 0 \\ 0 & 0 & 0 & 0 \\ 0 & 0 & 0 & 0 \end{bmatrix} \cdot \begin{bmatrix} a_{1,1} \\ a_{1,2} \\ a_{2,1} \\ a_{2,2} \end{bmatrix} = \begin{bmatrix} 0 \\ 0 \\ 0 \\ 0 \\ 0 \\ a_{1,1} \\ a_{1,2} \\ 0 \\ 0 \\ a_{2,1} \\ a_{2,2} \\ 0 \\ 0 \\ 0 \\ 0 \\ 0 \\ 0 \end{bmatrix} \quad (8)$$

Like last time, we only need to reshape back into given dimensions to obtain the result:

$$C = \begin{bmatrix} 0 & 0 & 0 & 0 \\ 0 & a_{1,1} & a_{1,2} & 0 \\ 0 & a_{2,1} & a_{2,2} & 0 \\ 0 & 0 & 0 & 0 \end{bmatrix} \quad (9)$$

If we were to now perform any convolution with kernel size $[2, 2]$ on C , our output will have size 2×2 , which matches the original image. Hence, performing appropriately-sized padding before a convolution will preserve the dimensions of the input and output.

In general, if we wish to perform a convolution with kernel size (k_1, \dots, k_n) on a tensor of order n and we wish for the output shape to match the input shape, we need to pad each dimension i with $k_i - 1$ entries on each side.

3.2 Skip connections

With resampling matrices and padding matrices now introduced, we can create CNNs with arbitrarily many skip connections, which can have many more layers, allowing for greater expressiveness.

In Section 2, we created feed-forward networks by composing matrices that represent successive layers and demonstrated that the result was an affine map. Here, we use a slightly different setup; instead of creating maps $\alpha^{(i)}$ that act as a single layer which we then compose together, we construct our network f recursively by defining maps $f^{(1)}, \dots, f^{(n)}$. We then take $f = f^{(L)}$. These maps are defined as follows:

$$\begin{aligned}
 f^{(0)}(X) &= X \\
 f^{(i)}(X) &= W^{(i)} P^{(i)} \left(\sum_{k=0}^{i-1} t^{(k,i-1)} R^{(k,i-1)} f^{(k)}(X) \right) + B^{(i)} \tag{10} \\
 &\text{for all } i \in \{1, \dots, L\}
 \end{aligned}$$

Here, for all i , we take $\{t^{(k,i)} : k = 0, \dots, i\}$ to be constants s.t. $\sum_{k=0}^i t^{(k,i)} = 1$. These represent the weights of our skip connections, and we use $i - 1$ as the second index since skip connections augment the *inputs* to each layer. For any pairs of layers k and i where we do not desire a skip connection, we simply set $t^{(k,i-1)} = 0$.

Note that we can also set $t^{(k,k)} = 0$, allowing for cases where a layer does not feed into the subsequent layer. This facilitates neural networks with many ‘paths’ (e.g. one path consisting of even-numbered layers and another for odd-numbered layers).

Each $R^{(k,i-1)}$ is a resampling matrix that resamples the dimensions of $f^{(k)}(X)$ to match the dimensions of $f^{(i-1)}(X)$ (which are the *input* dimensions for $f^{(i)}(X)$). Each $P^{(i)}$ is a padding matrix.

In practice, not every layer of a CNN would need to use both resampling matrices and padding matrices, since using one negates the necessity for the other. For any $P^{(i)}$ or $R^{(k,i-1)}$ that we do not wish to use, we can replace them with identity matrices. To retain generality, we will keep all resampling matrices and padding matrices in our calculations.

We can also add *batch normalization* into our toolkit, which scales inputs into each layer by multiplying and adding scalar values. This change is trivial, so we will ignore it in our equations for simplicity.

We can now make the following observation:

Claim 3.1 *Let f be a map corresponding to a linear CNN with arbitrarily many skip connections. Then $f(X)$ is an affine map.*

Proof. Induction on layers.

First, note that $f^{(0)}$ is clearly affine.

Next, assume that each of $f^{(0)}$ through $f^{(i-1)}$ are affine for some $i \in \{1, \dots, L\}$. Then $f^{(i-1)}$ is given by (10), and is an affine sum of affine maps, and is therefore affine.

Q.E.D.

This observation gives way to the following:

Theorem 3.1 *Let $f_W^{(i)}(X) := W^{(i)} P^{(i)} \left(\sum_{k=0}^{i-1} t^{(k,i-1)} R^{(k,i-1)} f^{(k)}(X) \right)$ be the same as in (10) with all bias terms removed. Also take $\mathbb{1}_{hw}$ to be the identity matrix of size $hw \times hw$, and take $\vec{0}$ to be the zero vector of length hw . Then the following holds:*

$$f(X) = f_W^{(L)}(\mathbb{1}_{hw})X + f^{(L)}(\vec{0}),$$

where f is the map given by a CNN with L layers and arbitrarily many skip connections, and where X is an $h \times w$ input matrix that has been reshaped into a vector of length hw .

Proof.

Induction on layers $i = 1, \dots, L$ to show that $f^{(i)}(X) = f_W^{(i)}(\mathbb{1}_{hw})X + f^{(i)}(\vec{0})$.

First, take layer $i = 1$. We have:

$$f^{(1)}(\vec{0}) = W^{(1)} P^{(1)} \left(t^{(0,0)} R^{(0,0)} f^{(0)}(\vec{0}) \right) + B^{(1)} \quad (11)$$

$$= W^{(1)} P^{(1)} \left(t^{(0,0)} R^{(0,0)} \vec{0} \right) + B^{(1)} \quad (12)$$

$$= B^{(1)} \quad (13)$$

Hence:

$$f^{(1)}(X) = W^{(1)} P^{(1)} \left(t^{(0,0)} R^{(0,0)} f^{(0)}(X) \right) + B^{(1)} \quad (14)$$

$$= W^{(1)} P^{(1)} \left(t^{(0,0)} R^{(0,0)} f^{(0)}(\mathbb{1}_{hw}) \right) X + B^{(1)} \quad (15)$$

$$= f_W^{(1)}(\mathbb{1}_{hw})X + f^{(1)}(\vec{0}) \quad (16)$$

Next, assume that $f^{(k)}(X) = f_W^{(k)}(\mathbb{1}_{hw})X + f^{(k)}(\vec{0})$ for all $k \in \{1, \dots, i\}$. Then:

$$f^{(i+1)}(X) = W^{(i+1)}P^{(i+1)} \left(\sum_{k=1}^i t^{(k,i)} R^{(k,i)} f^{(k)}(X) \right) + B^{(i+1)} \quad (17)$$

$$= W^{(i+1)}P^{(i+1)} \left(\sum_{k=1}^i t^{(k,i)} R^{(k,i)} \left(f_W^{(k)}(\mathbb{1}_{hw})X + f^{(k)}(\vec{0}) \right) \right) + B^{(i+1)} \quad (18)$$

$$= W^{(i+1)}P^{(i+1)} \left(\sum_{k=1}^i t^{(k,i)} R^{(k,i)} f_W^{(k)}(\mathbb{1}_{hw})X \right) \quad (19)$$

$$+ W^{(i+1)}P^{(i+1)} \left(\sum_{k=1}^i t^{(k,i)} R^{(k,i)} f^{(k)}(\vec{0}) \right) + B^{(i+1)} \quad (20)$$

$$= W^{(i+1)}P^{(i+1)} \left(\sum_{k=1}^i t^{(k,i)} R^{(k,i)} f_W^{(k)}(\mathbb{1}_{hw}) \right) X + f^{(i+1)}(\vec{0}) \quad (21)$$

$$= f_W^{(i+1)}(\mathbb{1}_{hw})X + f^{(i+1)}(\vec{0}) \quad (22)$$

Taking $i = L$, we obtain the theorem.

Q.E.D.

Theorem 3.1 allows us to pre-calculate $f_W^{(L)}(\mathbb{1}_{hw})$ and $f^{(L)}(\vec{0})$, allowing us to make predictions far faster. When making predictions using a trained model, we need only calculate $f(X) = WX + B$, where $W = f_W^{(L)}(\mathbb{1}_{hw})$ and $B = f^{(L)}(\vec{0})$.

In practice, this allows us to use the predictive power of arbitrarily complex LCNs with skip connections while requiring the resources of a single-layer perceptron when the trained model makes predictions.

4 Removing Skip Connections With a Homotopy

In this section, we present another method of reducing the computational resources for making predictions with CNNs. Unlike in Section 3, this method applies to both linear and nonlinear networks.

In (10), we gave a recursive definition for skip connections. In standard CNNs with skip connections, one would set $t^{(i-1,i-1)} = 0.5$ for all i , set $t^{(j,i-1)} = 0.5$ for at most one value of $j < i-1$, and set $t^{(k,i-1)} = 0$ otherwise. This would mean that the input to the i^{th} layer would be given by $0.5x^{(i-1)} +$

$0.5x^{(j)}$, where $x^{(i-1)}$ and $x^{(j)}$ are the padded and scaled outputs of the $(i-1)^{\text{th}}$ and j^{th} layers, respectively.

We can simplify this scenario by unifying all of our $t^{(k,i-1)}$ values into a single parameter that we simply call t . We then set the input to the i^{th} layer to:

$$t \cdot x^{(i-1)} + (1 - t) \cdot x^{(j)} \tag{23}$$

Note that when $t = 0.5$, we get the standard setup for skip connections, and when $t = 0$, we get a network with no skip connections. Hence, if we allow t to be a parameter of our model f , we see that $f(x, t)$ is a homotopy between skip connection models and feed-forward models. This allows us to train a model that utilizes the benefit of skip connections by starting at some $t_0 \in (0, 1)$, then reduce t as the model trains so that the final model is $f(x, 0)$.

By having no skip connections in the resulting model, we obtain reduced computation times and memory usage when making predictions.

For homotopies to work out numerically, the solution paths need to be free of singularities. In the setup of neural networks, randomness is introduced via the application of the stochastic gradient methods and we conjecture that this removes the difficulties caused by singularities. But this remains a subject of future study.

5 Computational Experiments

In Section 3 and Section 4, we introduced methods for obtaining improved prediction times. In this section, we use practical experiments to evaluate the speedup obtained with these methods, which are split across Subsections 5.2 and 5.3.

5.1 Equipment, Software, and Data

In both experiments, we use the MNIST database of handwritten digits with 60,000 labeled images for the training set, and 10,000 labeled images for the validation set. All models are built in PyTorch, and run on an NVIDIA GeForce RTX 2060 Mobile GPU. When we refer to prediction time, we record the mean wall clock time across an entire epoch of the dataset, without including any overhead (such as transforming data and loading the data into the GPU). We use a batch size of 64.

We also utilize **ResNet** – in particular, **ResNet34**, named as such because it has 34 convolutional layers – a model that is known to produce strong performance on image classification problems and can be trained relatively easily while having a deep architecture. **ResNet34** consists of ‘basic blocks,’ which are two 3×3 convolutions. Multiple basic blocks form a ‘layer,’ and there are four layers in total, plus one convolution before and after these layers. Each layer contains 3, 4, 6, and 3 basic blocks, respectively, giving a total of 34 convolutions, and each layer’s output has a skip connection to the subsequent layer’s input.

5.2 Pre-computing CNNs

In Section 4, we introduced a method to pre-compute CNNs with skip connections, reducing the computational requirements to that of a single-layer perceptron. To demonstrate the effectiveness of this reduction, Figure 1 compares the accuracy of various linear networks on the validation set of MNIST as the networks train. One of these networks is a modified version of **ResNet34** with all nonlinear ReLU activation functions removed (which results in a linear network), and the other network is as described in Section 3 with 3 convolutional layers and a skip connection from the first layer to the third layer. We see that both the 3-layer network and the linearized **ResNet34** produce better performance than the single-layer perceptron without sacrificing speed or memory when making predictions.

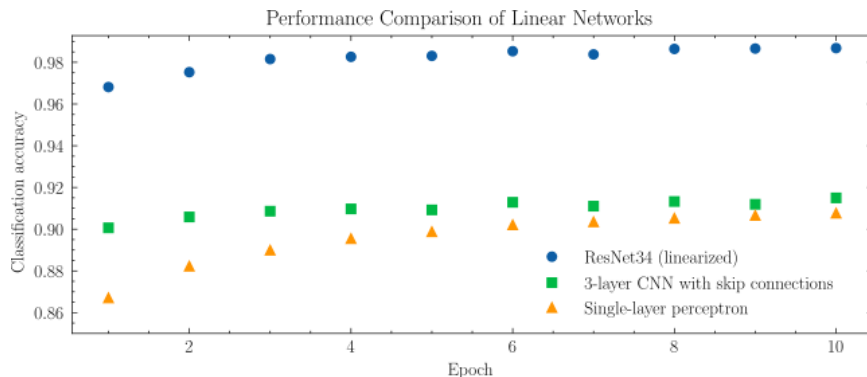


Figure 1: Classification accuracy for varying values of t (skip connection strength) in ResNet34. 10 epochs were performed over the MNIST dataset in each trial, and the mean result over 5 trials was taken for each point shown in the scatter plot.

We can also measure the speedup compared to a version of each of these models that have not been pre-computed. When averaged over 5 epochs, the mean prediction time for the linearized **ResNet34** for a single image is 104.91 microseconds. For a basic 3-layer CNN with skip connections, the mean prediction time is 12.05 μ s. Since both of these models fit the description of Theorem 3.1, they can both be reduced to single-layer perceptrons, which have a mean prediction time of 2.06 μ s. In the case of **ResNet34**, this is a speedup of over **98%**.

5.3 Practical experiment for removing skip connections

In this section, we compare the accuracy of a standard **ResNet34** against one that gradually has its skip connections removed, as described in Section 4. To achieve this, we need to set an initial value for t (let us call the initial value t_0), which then decreases as the model trains, before reaching 0 at the end of training. To decide on a suitable t_0 , we could either opt for the standard choice of 0.5, or we could refer to Figure 2, which shows average classification accuracy on the validation set across the first two epochs for various choices of t_0 . Using Figure 2, we see that values near (but not equal to) 1 produce high initial classification accuracies on the validation set, so we use an initial value of $t_0 = 0.9$.

It is worth noting that the shape of the graph in Figure 2 differs for other networks. For shallow networks, we observe roughly constant performance for values of t up to a certain threshold, before sharply dropping off — this is because shallow networks do not benefit as much from skip connections as deeper networks, and greatly suffer when the strength of skip connections is too strong, resulting in weak performance for high t values. On the other hand, for moderately deep networks, such as **ResNet18**, we observe an upside-down u-shaped curve, with moderate-strength skip connections performing best. Examples of such graphs can be seen in this project’s Github repository. In our case, with **ResNet34**, we observe the best performance with very high values of t because these allow the gradients to propagate through the network more easily, which is particularly important for deeper networks. $t = 1$ produces the worst relative performance because it severely reduces the expressiveness of the model by cutting out the skipped layers altogether.

With our initial value chosen, we have many choices for how to schedule t as we train. One simple option would be to set thresholds for validation accuracy that, when passed, result in a pre-specified, lower value of t . More advanced methods for scheduling other hyperparameters in deep learning, such as learning rate, have already been explored [12] and could be applied

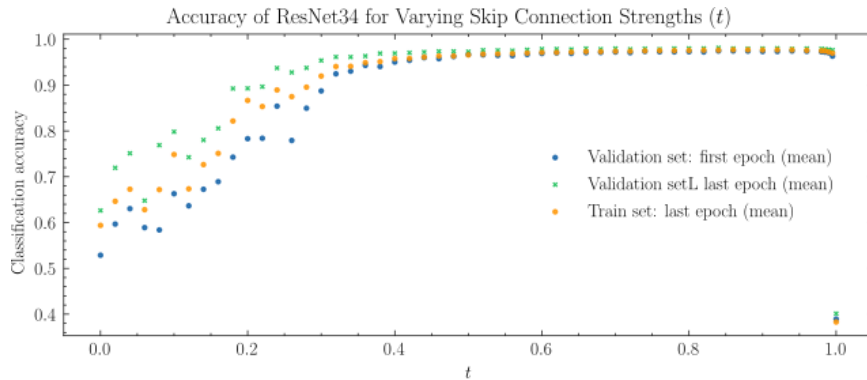


Figure 2: Classification accuracy for varying values of t (skip connection strength) in ResNet34. 2 epochs were performed over the MNIST dataset in each trial, and the mean result over 5 trials was taken for each point shown in the scatter plot.

to t too. However, to maintain simplicity and problem tractability, we opt for a method where we schedule different predetermined values of t for each epoch, allowing us to have a fixed number of epochs. In our case, we use 10 epochs, with corresponding values of t for each epoch set to $\{0.9, 0.7, 0.5, 0.3, 0.2, 0.1, 0.05, 0.025, 0.01, 0\}$ accordingly.

Figure 3 shows a comparison across 10 epochs with scheduled t values against a setup where we keep t static at 0.5 (which gives the standard setup with skip connections), with results averaged over 5 trials. We see that the model trained with a schedule for t does not significantly lose validation accuracy over the static model.

Figure 3 also shows another schedule starting at $t_0 = 0.5$: $\{0.5, 0.4, 0.3, 0.2, 0.1, 0.05, 0.025, 0.01, 0.05, 0\}$. This schedule is more representative of a situation where we do not know what value of t_0 would work best — this is often likely to be the case because it can be computationally expensive to produce results as in Figure 2. This schedule can be applied searching for a good t_0 , making it widely applicable. Again, we still do not observe any significant loss in accuracy.

To contextualize the speed difference when making predictions, we need only compare a version of ResNet34 that uses skip connections against one that does not. When averaged over 5 epochs of the MNIST dataset placed in batches of 64 running on an NVIDIA GeForce RTX 2060 Mobile, the mean time for a single prediction with ResNet34 is 106.83 microseconds. On the other hand, when skip connections are removed (by explicitly taking

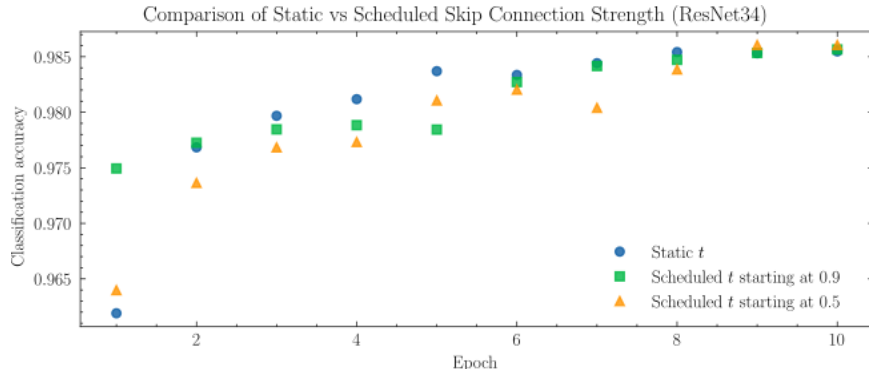


Figure 3: Classification accuracy of ResNet34 on MNIST validation set across 10 epochs using a ResNet34 model with (a) fixed t (skip connection strength) compared to (b) scheduled values of t that decrease to 0 (c) scheduled values starting at 0.5 that can be applied to other models. Each point shown is the mean over 5 trials.

their programming out of the network rather than simply setting $t = 0$), the average time is 83.1 microseconds. This is a speedup of approximately **22%**.

The speedup is even more stark for networks with more skip connections. By creating a basic 6-layer CNN as described in Section 2, a version with skip connections between all non-consecutive layers averages $30.72 \mu\text{s}$, compared to an average of $16.44 \mu\text{s}$ with skip connections removed, a **46%** speedup.

6 Future Directions

We have obtained two similar but distinct results; one showing that arbitrarily complex *linear* CNNs can be vastly simplified, and another showing that nonlinear CNNs can be lightly simplified. Unifying these two results would provide great computational improvements while leveraging the full expressiveness of nonlinear CNNs.

To achieve this, one would need to represent nonlinear functions of matrices efficiently. ReLU, along with all other piecewise linear activation functions (e.g. leaky ReLU and step functions), have been explored by Zhang, Naitzat, and Lim [22], who characterized neural networks using such activation functions with tropical geometry. By using this framework on LCNs with skip connections, one may be able to train nonlinear neural networks with skip connections that are later removed (as we have shown), before simplifying the network by pre-computing the transformation map from in-

put space to output space. This could involve pre-computing the model’s function on each of the distinct parts of function space into which the model divides the input plane into locally linear functions. In such a case, nonlinearities may need to be used sparingly to avoid dividing the plane an intractable number of times.

Another area of focus may be to apply more advanced methods of scheduling the skip connection strength parameter t . Previously-explored methods for scheduling the learning rate, parameter α (such as in [12]) could be adapted for use here with slight modifications, such as requiring that t eventually becomes sufficiently close to 0. Alternatively, since changing t also changes the model itself, we could view this approach as a form of *knowledge distillation* [4], one could use further techniques from this field to cut down the size of the network much more aggressively. This approach may even be combined with the tropical geometry approach to reduce the number of nonlinearities, resulting in a pre-computable and tractable model that preserves the teachers performance while reducing memory costs and computational costs.

References

- [1] Jiakang Bao, Yang-Hui He, and Edward Hirst. Neurons on amoebae. *Journal of Symbolic Computation*, 116:1–38, 2023.
- [2] Gergely Bércezi, Honglu Fan, and Mingcong Zeng. An ML approach to resolution of singularities. In *Topological, Algebraic and Geometric Learning Workshops 2023*, pages 469–487. PMLR, 2023.
- [3] Dorian Florescu and Matthew England. Constrained neural networks for interpretable heuristic creation to optimise computer algebra systems. *arXiv preprint arXiv:2404.17508*, 2024.
- [4] Jianping Gou, Baosheng Yu, Stephen J Maybank, and Dacheng Tao. Knowledge distillation: A survey. *International Journal of Computer Vision*, 129(6):1789–1819, 2021.
- [5] Moritz Hardt and Tengyu Ma. Identity matters in deep learning. In *International Conference on Learning Representations*, 2017.
- [6] Kaiming He, Xiangyu Zhang, Shaoqing Ren, and Jian Sun. Deep residual learning for image recognition. In *Proceedings of the IEEE conference on computer vision and pattern recognition*, pages 770–778, 2016.

- [7] Tianhao Hu, Bangti Jin, and Zhi Zhou. Solving Poisson problems in polygonal domains with singularity enriched physics informed neural networks. *arXiv e-prints*, pages arXiv–2308, 2023.
- [8] Yao Huang, Wenrui Hao, and Guang Lin. HomPINNs: Homotopy physics-informed neural networks for learning multiple solutions of nonlinear elliptic differential equations. *Computers & Mathematics with Applications*, 121:62–73, 2022.
- [9] Joe Kileel, Matthew Trager, and Joan Bruna. On the expressive power of deep polynomial neural networks. *Advances in neural information processing systems*, 32, 2019.
- [10] Kathlén Kohn, Thomas Merkh, Guido Montúfar, and Matthew Trager. Geometry of linear convolutional networks. *SIAM Journal on Applied Algebra and Geometry*, 6(3):368–406, 2022.
- [11] Thomas Laurent and James Brecht. Deep linear networks with arbitrary loss: All local minima are global. In *International conference on machine learning*, pages 2902–2907. PMLR, 2018.
- [12] Zhiyuan Li and Sanjeev Arora. An exponential learning rate schedule for deep learning. In *8th International Conference on Learning Representations, ICLR 2020*, 2020.
- [13] Shaowei Lin. *Algebraic methods for evaluating integrals in Bayesian statistics*. University of California, Berkeley, 2011.
- [14] Petros Maragos, Vasileios Charisopoulos, and Emmanouil Theodosis. Tropical geometry and machine learning. *Proceedings of the IEEE*, 109(5):728–755, 2021.
- [15] Emin Orhan and Xaq Pitkow. Skip connections eliminate singularities. In *International Conference on Learning Representations*, 2018.
- [16] Lynn Pickering, Tereso del Río Almajano, Matthew England, and Kelly Cohen. Explainable AI insights for symbolic computation: A case study on selecting the variable ordering for cylindrical algebraic decomposition. *Journal of Symbolic Computation*, 123:102276, 2024.
- [17] Maithra Raghu, Ben Poole, Jon Kleinberg, Surya Ganguli, and Jascha Sohl-Dickstein. On the expressive power of deep neural networks. In *international conference on machine learning*, pages 2847–2854. PMLR, 2017.

- [18] Sumio Watanabe. Almost all learning machines are singular. In *2007 IEEE Symposium on Foundations of Computational Intelligence*, pages 383–388. IEEE, 2007.
- [19] Sumio Watanabe. *Algebraic geometry and statistical learning theory*, volume 25. Cambridge university press, 2009.
- [20] Sumio Watanabe and Manfred Opper. Asymptotic equivalence of Bayes cross validation and widely applicable information criterion in singular learning theory. *Journal of machine learning research*, 11(12), 2010.
- [21] Haikun Wei, Jun Zhang, Florent Cousseau, Tomoko Ozeki, and Shun-ichi Amari. Dynamics of learning near singularities in layered networks. *Neural computation*, 20(3):813–843, 2008.
- [22] Liwen Zhang, Gregory Naitzat, and Lek-Heng Lim. Tropical geometry of deep neural networks. In *International Conference on Machine Learning*, pages 5824–5832. PMLR, 2018.